STRUCTURAL INTEGRITY ASSESSMENT OF PIPES FOR HIGH TEMPERATURE APPLICATIONS

[1]Antonietta Lo Conte, Federico Bassi, Roberto Sanfilippo
[1]Politecnico di Milano, Department of Mechanical Engineering, I-20156 Milano, Italy
[2]Mihaela Eliza Cristea, Caterina Turconi
[2]Tenaris Dalmine, R&D, I-24044 Dalmine, Italy

ABSTRACT

The aim of this paper is to study creep initiation and creep crack growth in grade P/T91 seamless tube, used in the manufacturing of power plants, and also to propose a methodology, based on these studies, to predict residual life of these components.
Creep Crack Growth tests have been conducted at 600 °C and different load levels on C(T) specimens. The initiation time, corresponding to an increase of the crack size Δa=0.2 mm, has been measured and initiation stress intensity factor has been obtained, as required by the Two Criteria Diagram approach in order to assess crack initiation. The applicability of the different parameters proposed to describe the creep crack growth behavior has been also validated. According to these results an assessment procedure, based on the sequential application of the Two Criteria Diagram for crack initiation and Nikbin-Smith-Webster model for crack propagation, has been proposed and applied to estimate the remaining lifetime of P/T91 piping products, at the typical service temperature of 600 °C, in case of an imperfection size postulated at the threshold of NDT control.

INTRODUCTION

The worldwide demands of power generation industries such as process cost reductions, high efficiency and flexibility in operating and maintaining the plants lead to the necessity of adequating remaining life assessment at elevated temperatures for engineering components. In particular, the continuous trends of higher operating temperatures combined with the extending life of existing power plants requires consistent experimental investigation as well as analytical approaches able to predict material behavior under operating conditions.
Considering both design codes, which generally consider defect free structures [1], and assessment codes [2-5] which address flaws and their treatment, European and International programs have been undertaken in collaboration with various power generation industries. A detailed description of these collaborative programs, their objectives and findings can be found in [6], where the historical and currently technical concepts are reported.
Regarding to the concepts applied to defect assessment, the treatment of high temperature failure emphasizes the need for reliable data for design and in-service assessment. In particular, the material characterization should be based on a sufficiently large experimental database, which consists of creep and creep crack growth tests lasting sufficiently long. Moreover, another important key point is the data transferability from specimens with different sizes to larger components with similar crack tip condition.
Finally, loading situation such as operating under high temperature and cyclic loads due to rapid load changes or fast startups must also reflect in the design of such engineering components. Standard procedures [1] are applied when damage for creep and fatigue occurs separately during plant operation. Combined circumstances when fatigue and creep damage can commonly interact lead to unexpected onset of cracking and consequently reduced component endurance. Furthermore, complex situations when startups lead to rapid increase on key operating parameters, including temperature, pressures and mass flow, can generate high thermal stresses, mainly due to the uneven temperature distribution. This can be translated into an increased level of component stress, which has often an adverse effect on material degradation and component life.
Under this difficult scenario, the understanding of materials response to thermal-mechanical stresses, creep crack growth, creep-fatigue damage mechanics and their interactions becomes extremely important for the development and application of reliable assessment models.
For these purposes, the present paper deals with the understanding and prediction of creep crack initiation (CCI) and growth (CCG) of P/T91 steel grade by means of defect assessment procedures on both small and full scale. In particular, the used approaches for CCI and CCG are based on methods able to take into consideration similitude concepts with the aim of life prediction of components. In particular, Two Criteria Diagram (2CD) approach has been used for creep crack initiation assessment, and Nikbin-Smith-Webster model (NSW) for creep crack growth, which allows the use of reference stress for both small scale specimens as well as ‘global’ collapse solution for components.
The models based on experimental data, required creep crack growth tests according to ASTM Standard [11] which have been performed on C(T) half inch specimens. The online monitoring by the electrical potential drop technique allowed us to identify the two stages of creep crack initiation and growth data.
The initiation time, corresponding to an increase of the crack size Δa=0.2 mm, has been measured and the initiation stress intensity factor has been obtained, as required by the Two Criteria Diagram (2CD) approach in order to assess the crack initiation. The 2CD well describes the initiation condition in the examined material and it is proposed as method to transfer creep crack initiation data, from specimens with different size to larger components with similar defect characteristics and crack tip situation.

The applicability of the different parameters proposed to describe the creep crack growth behavior has also been validated. According to Nikbin-Smith-Webster (NSW) creep crack growth model, the crack growth rate of P91 experimental test results are well correlated by a power of the fracture mechanics parameter C*. The coefficients of the NSW model have been obtained on the basis of the experimental data, and the NSW model has been proposed to describe the crack growth rate on the component.
According to these results an assessment procedure, based on the sequential application of the 2CD for crack initiation, and NSW model for crack propagation, in order to estimate the remaining lifetime of P/T91 piping products, at the typical service temperature of 600 °C, in case an imperfection is postulated with depth within the threshold of NDT control is hereby proposed and applied.
CCG experimental results as well as material creep behavior allowed to extend the assessment procedure to perform assessment of components in presence of defects and to determine the remaining lifetime conditions also in creep fatigue conditions.
The final aim of the paper is the analysis of a case study in order to discuss the transfer of material crack initiation and crack growth rate data to the behavior of complex structures. The proposed assessment procedure for high temperature component is applied to the evaluation of the residual life of a standard pipe product with an initial imperfection.
The component object of the proposed case study is also calculated according to the approach proposed by the API/ASME Code [23] and the results of the two different procedures are compared.

MATERIAL

Creep behavior

The design process for the life prediction of components at high temperature is based on creep data set including stress, temperature, secondary creep rate, and time to failure. Accurate evaluation of uniaxial creep strength is the first important issue to ensure safety and reliability of these components.
Typically, experimental data are available for test duration up to 10^5 hours [7-10], while the service of the component is often required for $2 \div 3\ 10^5$ hours. Several parametric equations are documented in literature to represent the secondary creep rate and the failure time relationships with temperature and stress. These may be fitted empirically to experimental data and extrapolated to longer duration.
For P/T91 grade at 600 °C, investigated in this paper, a representative set of experimental data have been collected and analyzed to describe the uniaxial rupture and creep deformation behavior.
In order to represent the relationship between stress, temperature and time to failure, Larson & Miller parameter was used:

$$P_{LM} = T*\left(C + \log t_R\right) \tag{1}$$

where T is the temperature in K, t_R is the time to failure in hours and C is a constant, and the hypothesis that the plot of log t_R versus 1/T results in converging straight lines at each stress level is assumed to be valid. The use of this parameter enables all stress rupture data to be plotted on a master curve where data at low temperatures and long time to failure are equivalent to data at high temperature and shorter time to failure. The plot of the Larson Miller parameter (PLM) and its scatter band is given in Fig. 1 for tests at 600 °C and for a range of the stress level restricted to the values of interest at this temperature.

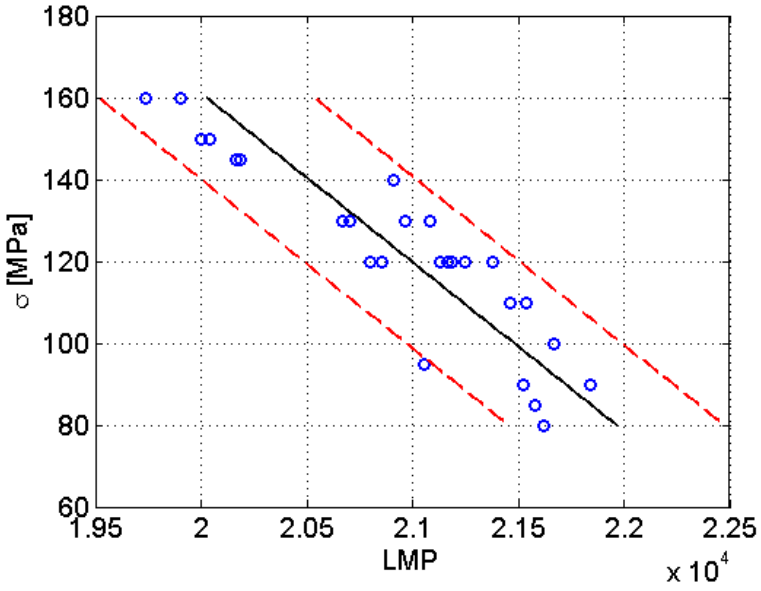

Figure 1: Larson-Miller Parameter with trend line and 95% confidence intervals at 600 °C.

Fig. 2 shows the secondary creep rate $(\dot{\varepsilon}_{\min})$ plotted versus the applied stress (σ). The secondary creep rate as function of the stress results is represented by Norton's power law:

$$\dot{\varepsilon}_{\min} = A\sigma^n \tag{2}$$

with the value of the stress exponent *n* and constant *A* depending on the testing conditions. In particular, a bilinear trend can be observed, at low stress level n is about 4; while at higher stress level, when dislocation creep is operative, a difference in creep behavior is observed and n is about 16.

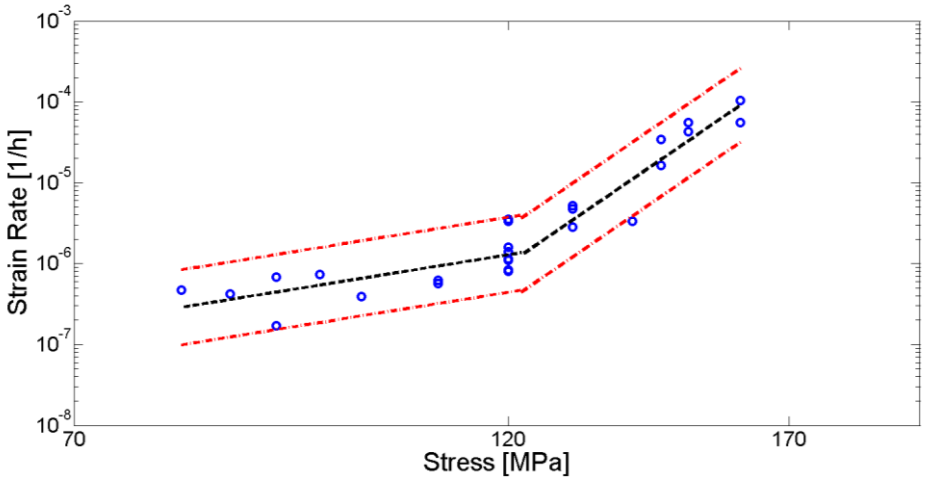

Figure 2: Strain rate as a function of stress with trend line and 95% confidence intervals at 600 °C

CCG tests

CCG test have been performed on C(T) specimens with width W = 25.4 mm and B = 12.7 mm according to ASTM E1457 [11]. All the specimens were fatigue pre-cracked at room temperature under the condition of a load ratio R=0.05. The lengths of the fatigue pre-cracks were about 1.6 mm. The tests were performed at constant load at 600 °C with temperature control for all the specimens within ±1 °C. Creep crack length was measured by DC electrical potential drop method with the configuration for the electrical leads shown in Fig. 3. To convert electrical potential drop into crack length, the calibration equation derived in [12] for the ½ inch C(T) specimen was used.

Normalized results of crack length versus time are reported in Fig. 4 for different value of the nominal stress intensity factor. At the end of the CCG tests each specimen has been broken in liquid nitrogen and the fracture surface has been examined. The fatigue crack length and the creep crack growth have been measured according to the scheme of Fig. 5 in order to validate the potential drop measurements of the crack length. Moreover, for each crack growth test, the data of crack length versus time have been analyzed in order to obtain the time of crack growth initiation (t_i) and the crack growth rate *da/dt*. The time of crack growth initiation is defined as the time at which a significant crack growth, taken equal to 0.2 mm, has been reached. From this graphs, and the corresponding load, also the value of the parameter K_{Ii} that characterizes the creep crack initiation of the material can be obtained. An important feature of the parameter K_{Ii} is that data converge on a linear trend, if plotted in logarithmic scale versus the initiation time (t_i), as shown in Fig. 6 .

Crack growth rate can be expressed as a function of crack length of time and correlate to an appropriate parameter to characterize the creep crack growth behavior of this material on the present activity load conditions. The theory behind the correlation of high temperature crack growth data essentially follows that of elastic-plastic fracture mechanics. The crack tip stress and strain rate fields of ductile materials under steady crack growth are characterised by the parameter C* which can successfully correlate creep crack growth. The C* parameter is defined as the stabilized value of the parameter *C(t)* for t→∞, i.e. when the effect of creep caused the complete redistribution of stresses behind the crack tip:

$$C^* = C(t \to \infty) = \int_\Gamma \dot{W}(t)dy - T_i \frac{\partial \dot{u}}{\partial x} ds \tag{3}$$

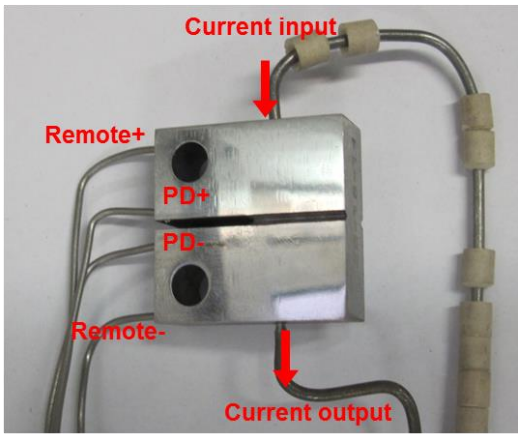

Figure 3: The specimen with the potential leads on the left and the current leads on the top and bottom surface of the specimen.

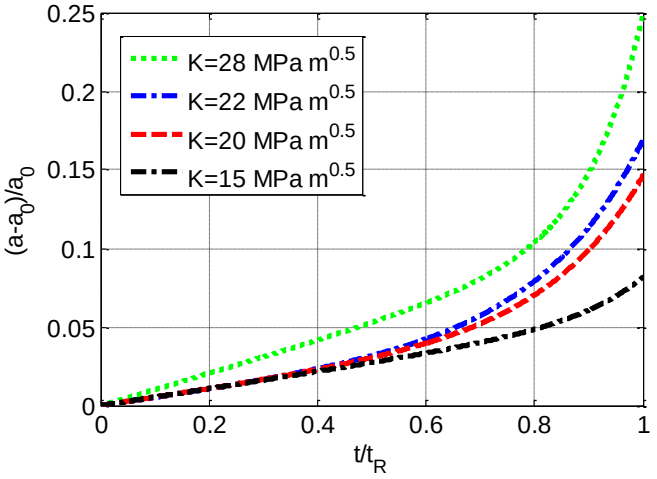

Figure 4: Crack length versus time for different value of the nominal stress intensity factor.

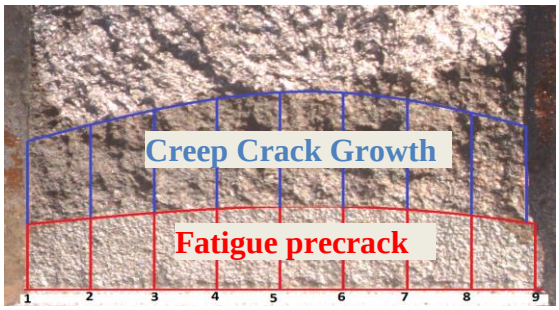

Figure 5: Fracture surface after Creep Crack Growth tests and schematic for crack length measurements.

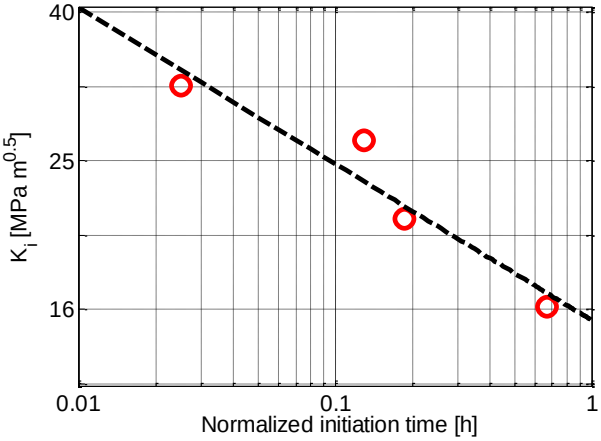

Figure 6: Parameter K_{Ii} versus the initiation time (normalized).

where Γ is a contour around the crack tip, $\dot{W}(t)$ the strain energy density rate, *Ti* the components of the traction vector and $\dot{u}_i$ are the components of the displacement rate vector. By analogy between steady state creep and plasticity, the integral (equation 3) is independent from the path Γ when elastic strain rates are negligible throughout the body.
Once a steady-state distribution of stress and creep damage has been developed ahead of a crack tip, it is usually found that creep crack growth rate can be described by an expression of the form [13]:

$$\frac{da}{dt} = DC^{*\phi} \tag{4}$$

where D and ϕ are material constants. Nikbin et al. [14] demonstrated that the power dependence of C* varies only over the range 0.7-1 and the crack growth rate can be predicted by:

$$\frac{da}{dt} = \frac{3 \cdot C^{*\frac{n}{n+1}}}{\varepsilon_f^*} \tag{5}$$

where n is the stress exponent of the Norton law and ε_f^* is the multiaxial creep ductility.

Equation 5 represents the NSW Model and is also included in the statement of the BS 7910 rule [2] for the estimation of the creep crack propagation ratio in components operating at high temperature. In this model the extremes of plane stress

and plane strain conditions are predicted taking into account the decrease of creep ductility under multiaxial stress conditions (ε_f^*), with respect to the uniaxial creep ductility (ε_f).

In order to verify the validity of the NSW model for the examined material, the parameter C* can be determined by experimental tests of CCG based upon the load line creep displacement rate, $\dot{\Delta}^c$,

$$C^* = \frac{P\dot{\Delta}^c}{B\,b} F \tag{6}$$

where P is the applied load, b is the remaining ligament ahead the crack tip, B is the net thickness, and F is a factor dependent on crack length, specimen geometry and stress exponent of the Norton law n.

From experimental CCG tests it has been found that if the proper uniaxial creep ductility of the material is assumed equal to 0.25, as average values obtained from uniaxial creep tests at 600° C, and the ratio $\varepsilon_f^* / \varepsilon_f$ is assumed equal to 1/7 as proposed in [14], the creep growth rate predicted by the NSW model in plane stress and plane strain conditions (Equation 5) well represents the lower and upper bound of the crack propagation ratio versus C* for the investigated material (Fig. 7). The dependence of crack growth rate da/dt on C* parameter follows a near linear trend on log-log scale with a relative narrow scatter band. It indicates that crack growth rate correlates with C* parameter according to equation 5, and that the C* parameter is appropriate to describe the crack growth of this material.

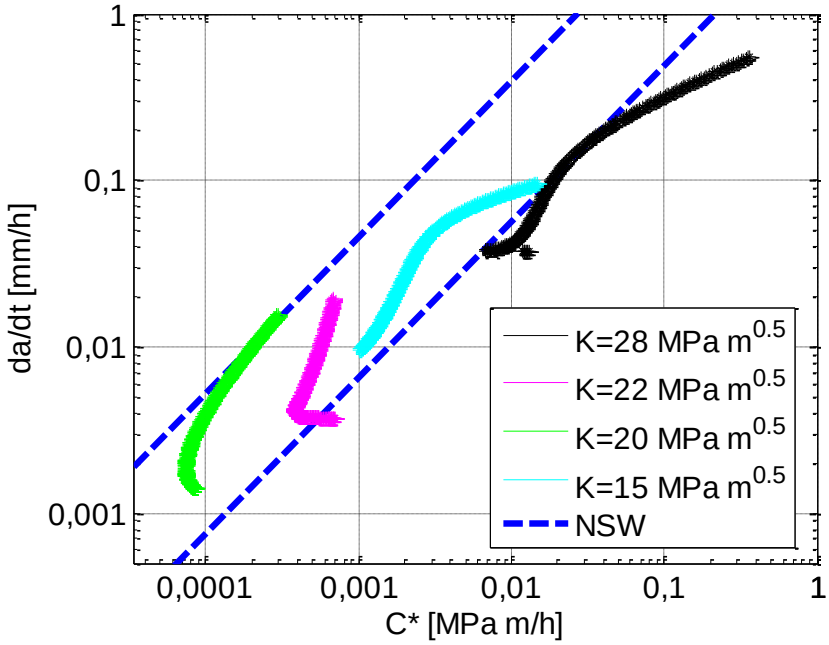

Figure 7: Normalized relationship between creep crack growth rate and C parameter.*

Short versus long tests

Experimental creep crack initiation and creep crack growth data are essential to assess the reliability of components operating at high temperature. The presented creep crack growth tests have been obtained on C(T) specimens which are a high constraint geometry, and are of relatively short duration, less than 3000 h. Therefore, results have been obtained within a practicable time scale (approximately 1 year). This means that the load applied to the specimen is relatively high and generates a reference stress in excess of the yield stress of the material, which implies that significant plasticity is introduced into the specimens on loading with a constraint loss effect. Recently [15] CCG of duration exceeding 16000 hours (long term tests) have been performed on C(T) specimen.

Results have shown that long-term C(T) specimens, characterized by the stress state at the crack tip with high constraint, experience a higher creep crack growth rate for a given value of C*, compared to short-term tests, where the constraint loss effect occurs. The creep toughness increases with reducing constraint and it is therefore non conservative to use data obtained from tests at low level of constraint for assessment where constraint is high.

In terms of C* value, the conditions in industrial components are actually represented by low C* value that also means high constraint. Under these conditions, the extrapolation of crack growth rate versus C* may be questionable.

Thus, additional longer-term tests on high constraint C(T) geometry would be beneficial to understand the behavior of the present material at lower value of initial stress intensity factor, and C* parameter during stationary creep crack growth. To save time, tests can be interrupted when the stationary crack growth rate is well established.

HIGH TEMPERATURE ASSESSMENT

For design and safety assessment purposes it is often necessary to establish the significance of imperfection in components subject to creep and creep-fatigue loading. In this section a simplified method to be used in practical assessment procedures of tubular product at high temperature is proposed. The method is based on experimental CCI and CCG data and represents the first step of a more general procedure of creep-fatigue assessment of such class of power plants components. The behavior of a postulated imperfection is described as a sequence of two stages. By analogy with CCG tests, the first stage is an incubation period where the creep damage builds up in front of the crack tip, but no significant crack growth occurs. The time that the crack reaches 0.2 mm is assumed as the starting time of the crack propagation (initiation time).The following stage is a steady state crack process taking a propagation time. The crack propagates through the material with cracking speed nearly constant until the maximum acceptable size is reached. The admissible exposure time of the component at 600 °C is thus calculated as:

$$t_{\exp osure} = t_{initiation} + t_{propagation} \tag{7}$$

Data required for the assessment are: operating conditions; the geometry of pipe and imperfection; creep and creep crack growth material data. The transfer of material data to account for multiaxial stress conditions is based on a simplified structural analysis to calculate the reference stress of the pipe for primary load [2].
Figure 8 shows the geometrical configuration of the pipe proposed as case study for the application of the assessment procedure. As service conditions, a temperature of 600 °C and two cases of internal pressure of 25 and 50 MPa are assumed.

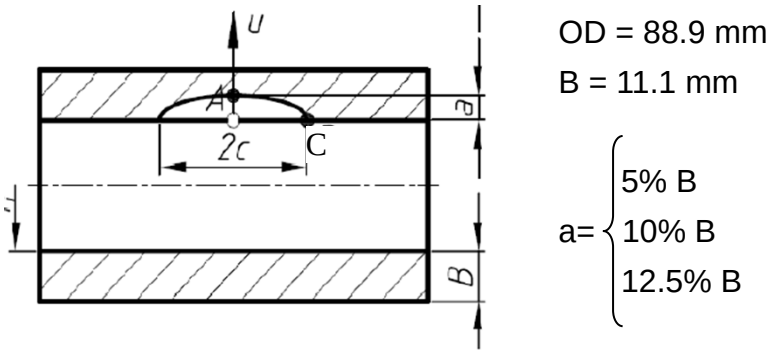

Figure 8: Geometry of the defected P/T91 pipe proposed as case study.

Initiation time

Two Criteria Diagram (2CD) has been developed for the assessment of crack initiation in components where ligament damage and crack tip damage are competitive process in determining the critical level of damage at the crack tip [17]. The 2CD is shown in Fig. 9.
In the 2CD for creep crack a load parameter for each type of damage is considered. The nominal stress $\sigma_{n,pl}$, i.e the reference stress in the component, considers the stress situation in the ligament and the nominal elastic stress intensity factor K_{Iid}, at time zero, describing the condition at the crack tip. The nominal stress normalized with respect to the stress for creep failure at the same temperature identifies the stress ratio:

$$R_\sigma = \sigma_{\text{n pl}} / \sigma_{\text{R}} \tag{8}$$

and the nominal elastic stress intensity factor K_{Iid} normalized with respect to the stress intensity factor at the initiation for the examined temperature ($K_{Ii,}$ in Fig. 6) identifies the stress intensity ratio:

$$R_K = K_{\text{I id}} / K_{\text{Ii}} \tag{9}$$

While R_k considers the presence of a defect in the component, R_σ just take into account the creep effects on smooth specimens away from possible defects. The 2CD defines three mechanisms of damage responsible for crack initiation. A low value of the ratio K_{Iid}/σ_{npl} indicates the beginning of the propagation due to the widespread damage in the resistant section behind the crack tip, a high ratio K_{Iid}/σ_{npl} indicates the initiation of the propagation due to localized damage of the crack tip, while between these extremes a transition zone indicates initiation due to a mixed damage mode. Crack initiation can only be expected above the crack-no crack boundary line (blue line of Fig. 9).

In this diagram the initiation conditions for the experimental CCG tests are reported. As the reference stress is higher than the stress for creep failure, but the nominal stress intensity factor is close to the stress intensity factor at the initiation, a mixed mode damage occurs (see Fig. 9).
In order to apply the 2CD for the estimation of the initiation time of the component, the following parameters have been evaluated at points A and C of Fig. 8:

- time corresponding to the boundary line of the ligament damage zone, given the value of $\sigma_{ref} = \sigma_{n,pl}$, the temperature and the Larson Miller plot of the material;
- time corresponding to the boundary line of the crack tip damage zone, given the value of the nominal stress intensity factor, the temperature and from CCG tests;
- time corresponding to the boundary line of the mixed mode damage, given the value of $\sigma_{ref} = \sigma_{n,pl}$, the nominal stress intensity factor, the temperature, the Larson Miller plot of the material, and the stress intensity factor at the initiation against the initiation time.

For each imperfection size the initiation time is defined as the minimum of the initiation time corresponding to each type of damage. Results are summarized in Table 1, where the initiation time is in red and results related to initiation of propagation at point A of Fig. 8.

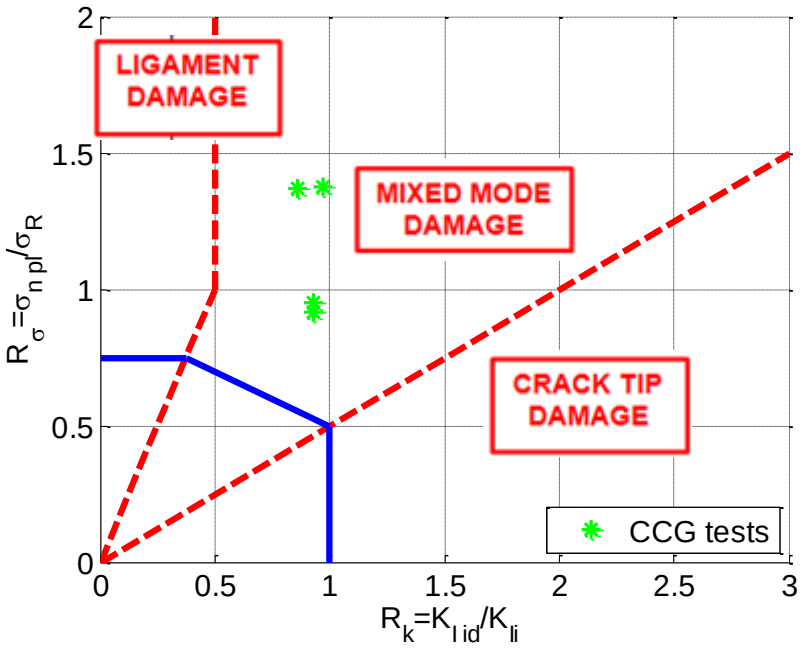

Figure 9: Two criteria diagram for crack initiation time.

Table 1: Summary of the predicted initiation time for each type of damage and for each imperfection size of Fig.8. The actual initiation time for each defect size is in underlined format.

Imperfection size	*Ligament damage*	*Mixed mode damage*	*Crack tip damage*
5% B	38251 h	20880 h	513285 h
10% B	38251 h	12981 h	124511 h
12.5 % B	38251 h	10745 h	76116 h

Crack propagation

Following initiation, creep crack growth versus time is built by integration of equation 5 that successfully relate crack growth rate in experimental tests, although such approach at low values of C* needs to be validated, as discussed in the section before.
In equation 5 C* is obtained as [2];

$$C^* = \sigma_{ref}\,\dot{\varepsilon}_{ref}\left(\frac{K}{\sigma_{ref}}\right)^2 \tag{10}$$

where $\dot{\varepsilon}_{ref}$ is defined by the Norton creep low for secondary creep rate and K is the stress intensity factor evaluated according to [19] for the crack size history at time t, under the reference stress (σ_{ref}) based on the nominal wall thickness [20].
Fig. 10 shows the crack propagation versus time until the maximum acceptable size, set at 85% of the thickness, is reached. The analysis were carried out for low loading case (25 MPa internal pressure) and mean trend of the material reported in Fig. 2. For all three imperfection sizes the admissible exposure time results higher than 10^5 hours.

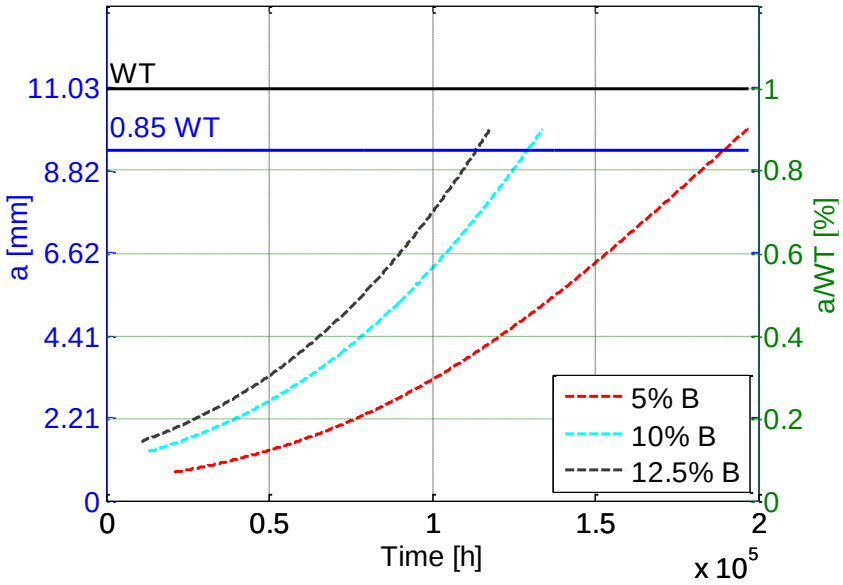

Figure 10: Crack propagation versus time for geometry and imperfection size of Fig. 8.

The reference stress approach of equation 10 to evaluate C* parameter is based on the hypothesis that the damage of the structures can be calculated as the damage in the uniaxial test at the appropriate stress level defined as the reference stress of the structure. Different methods to evaluate the reference stress, depending on the yield criteria employed to set the collapse condition, can lead to different results in terms of residual life of the component. Fig. 11 reports the crack propagation for imperfection size equal to 5% B as a function of time when a different method to evaluate σ_{ref}, global and local approaches, based on the collapse mechanism of the thinnest wall thicknesses [21, 22] have been applied. It is evident from Fig. 11 that that estimates of *C** determined from these reference stresses result in the largest *C** values and greatest crack growth rate. In contrast, the use of nominal wall thickness [20] results in a conservatism reduction.

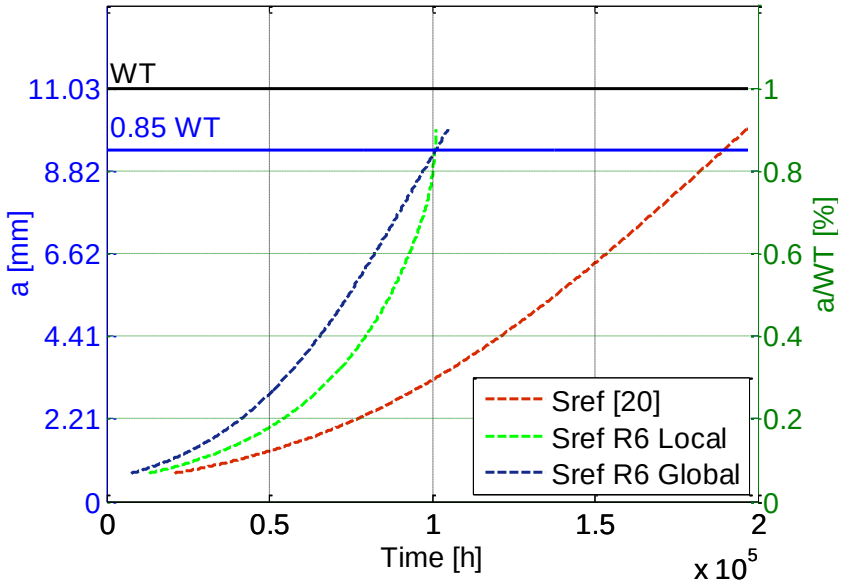

Figure 11: Crack propagation versus time for imperfection size equal to 5% B and different methods to evaluate σ_{ref}.

DISCUSSION OF THE RESULTS

The crack propagation of the case study of Fig. 8 has also been analyzed according to the approach of the API/ASME Code [23].
In this case the crack growth rate is computed using as crack driving force the C_t integral defined as:

$$C_t = C^* \left[\left(\frac{t_{relax}}{t} \right)^{\frac{n-3}{n-1}} + 1 \right] \tag{11}$$

where n is the stress exponent and

$$C^* = \frac{\dot{\varepsilon}_{ref}}{1 - D_{BC} - D_{AC}} \left(\frac{K}{\sigma_{ref}} \right)^2 \tag{12}$$

with D_{BC} and D_{AC} the damage before and after cracking respectively, obtained by application of the MPC Omega project method. The method evolved from examination of experimental data of improved database of creep range material properties, that was then converted to parametric expressions for easy calculation and extrapolation of time to failure and strain accumulation, as function of stress, temperature and mode of loading [23, 24].
To estimate the remaining life of the pipe after the crack initiation the creep crack growth rate is related to the C_t using equation (13) analogous to equation (5):

$$\frac{da}{dt} = HC_t^{\mu} \tag{13}$$

where the parametric approaches applied in the Omega Method are also used for generation of the parameters H and μ dependent on the uniaxial creep behavior of the material and the related scatter.
Figures 12a and 12b shows the predicted ASME/API crack propagation versus time for the imperfection size equal to 5%B for low and high loading condition, 25 and 50 MPa internal pressure respectively. The lower and upper bound account for the material scatter band. The same input parameters: imperfection size at 5%B, low and high loading conditions, as well as experimental material scatter band of the investigated grade, have been used for the predictions based on NSW Model reported in figures 13a and 13b.
It is evident that the predictions based on the average experimental material data are in good broad agreement with the prediction of the API/ASME based on the average uniaxial creep properties of the material for low stress condition, that is the one closer to high life service. For high stress condition, a more conservative prediction has been found when API/ASME code is applied.
However, the scatter band of Fig. 12a and 12b allows us to highlight the importance of experimental creep database on the investigated material, as well as creep crack growth parameter, in order to enhance the reliability of the remaining life prediction. A reduction of the working window by a factor of approximately 2 can be obtained for both low and high loading conditions.

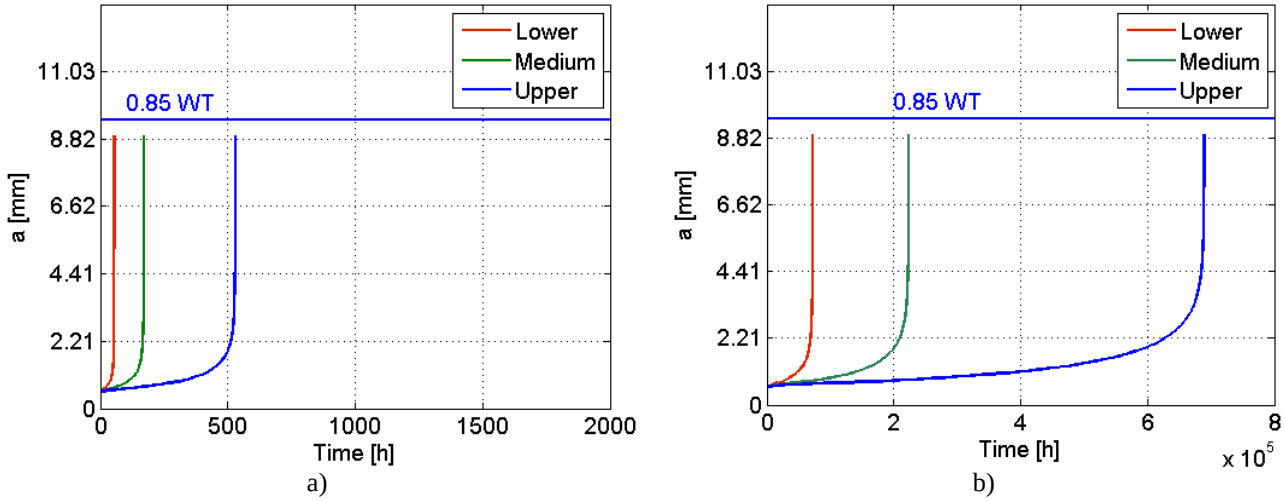

Figure 12: Crack propagation versus time for imperfection size equal 5% B according to ASME/API Code [23]: high stress a) and low stress b).

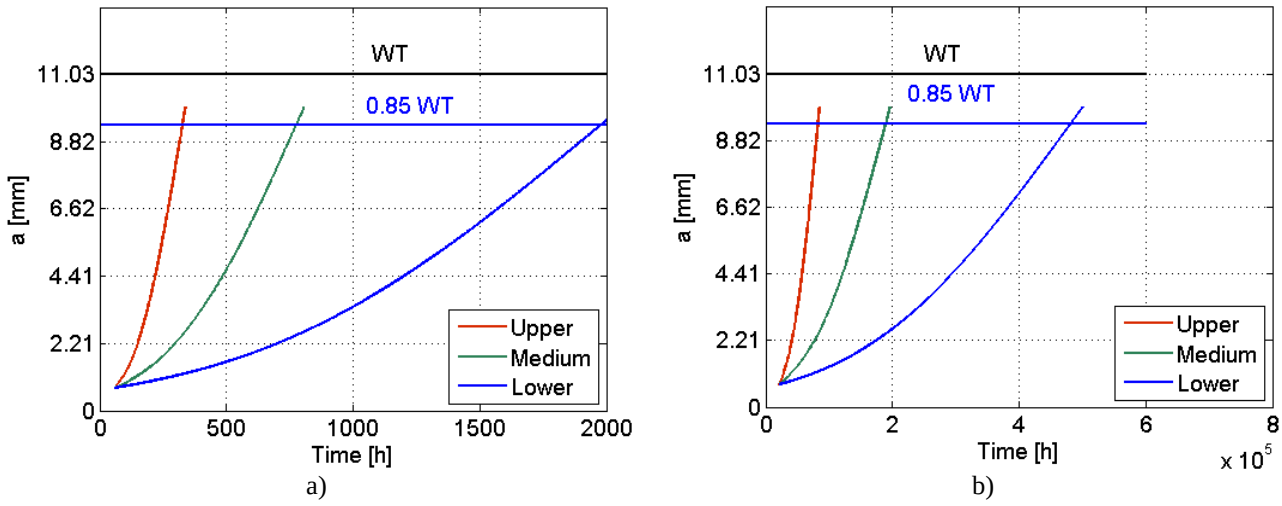

Figure 13: Crack propagation versus time for imperfection size equal 5% B according to NSW Model: high stress a) and low stress b).

CONCLUSIONS

Data on creep crack growth from P/T91 C(T) specimens at 600 °C have been measured and reported. The condition of the initiation of the stable propagation has been characterized in terms of stress intensity factor K_{Ii} that converges on a linear trend, if plotted in double logarithmic scale versus the initiation time (t_i).
The dependence of crack growth rate da/dt on C* parameter follows a near linear trend on log-log scale with a relative narrow scatter band. It indicates that crack growth rate correlates with C* parameter and the C* parameter is appropriate to describe the crack growth of this material.
Creep crack growth assessment procedure for pipe operating at high temperature has been described with particular attention to perform case involving initiation and stable propagation. On the basis of the experimental Larson-Miller parameter and data of initiation stress intensity factor, the initiation of crack propagation in a defected pipe has been predicted by means of the Two Criteria Diagram, while the experimental creep crack growth-C* parameter correlation has been used to predict the crack growth versus time. It has been shown that estimates of C* parameter for the component, and as consequence the estimate of the crack growth versus time, are sensitive to the formula used for calculating the reference stress, and the dimensions assumed for the wall thickness of the pipe.
Validation of the procedure, based on creep and creep crack growth data of the examined material, has been illustrated by comparison with ASME/API high temperature assessment procedure, that employs the parametric Omega Method approach to model the material behavior in the creep range.
It has been found good agreement about the remaining life prediction of the proposed procedure, with σ_{ref} based on the collapse mechanism of the nominal wall thicknesses, and experimental data of the T/P91 material, when comparisons are made with the estimation of the ASME/API method, based on the MPC Omega Project average creep properties of the material. However the scatter band of the crack propagation versus time for imperfection size equal 5% B according to the ASME/API Code and the scatter band in the related life prediction ($7.2\ 10^4 \div 7\ 10^5$) allows us to highlight the importance of experimental creep and creep crack growth parameter of the material in order to enhance the reliability of the remaining life prediction of the component.

ACKNOWLEDGMENTS

Dr. Mario Rossi, director of Tenaris Dalmine Research and Development Center, is kindly acknowledged for the permission to publish this paper.
The authors are especially grateful to prof. Stefano Beretta from Politecnico di Milano, and Dr. Ettore Anelli from Tenaris Dalmine R&D for the instructive suggestions and support during the development of the present work.

REFERENCES

[1] ASME Section III, Rules for construction of nuclear power plant components, Division 1, Subsection NH, Class 1 components in elevated temperature service, ASME, 1995.

[2] British Standard BS7910, “Guidance on methods for assessing the acceptability of flaws in metallic structures”, British Standards Institution, 2000.
[3] R5, “Assessment procedure for the high temperature response of structures”, Ed. Goodall I.W., British Energy-UK, Issue 2, 1998.
[4] A16, “Guide for Leak Before Break Analysis and Defect Assessment” RCC-MR, Appendix A16, Edition 2002, AFCEN No: 94-2002.
[5] FITNET, ‘Fitness for service analysis of structures using the FITNET procedure; An Overview’, 24th Int. Conf. on Offshore Mechanics and Artic Engg., Greece 12-17 June 2005.
[6] K. Nikbin, Creep/Fatigue Crack Growth Testing, Modelling and Component life assessment of welds, 6th International Conference on Creep, Fatigue and Creep-Fatigue Interaction [CF-6], Procedia Engineering 55 (2013) 380 – 393
[7] P. J. Ennis and A. Czyrska-Filemonowicz. Recent advances in creep-resistant steels for power plant applications. Sadhana, 28(3-4):709, 2003.
[8] HIROMICHI HONGO, MASAAKI TABUCHI, and TAKASHI WATANABE, “Type IV Creep Damage Behavior in Gr.91 Steel Welded Joints”, The Minerals, Metals & Materials Society and ASM International 2011.
[9] Y. Takahashi, International Journal of Pressure Vessel and Piping, 85 (2008), 406-422.
[10] P. Lombardi, Modellazione costitutiva e meccanica del danneggiamento di acciai 9% Cr per applicazioni ad alta temperatura, PhD thesis, Università di Cassino
[11] ASTM. “ASTM E 1457-07: Standard Test Method for Measurement of Creep Crack Growth Rates in Metals”, 2007.
[12] G. Belloni, E. Gariboldi, A. Lo Conte, M. Tono and P. Speranzoso, On the experimental calibration of potential drop system for crack length of compact tension specimen measurements, 2002, Journal of Testing and Evaluation, volume 30, pp.461-469
[13] J. Ha, M. Tabuchi, H. Hongo, A. Toshimitsu Jr, A.Fuji, Creep crack Growth properties for 12CrWCoB rotor steel using circular notched specimens, International Journal of Pressure Vessels and Piping, 81 (2004), 401-407.
[14] S. Maleki, Y. Zhang, K. Nikbin, Prediction of Creep Crack growth properties of P91 parent and welded steel using remaining failure strain criteria, Engineering fracture Mechanics 77(2010), 3035-3042.
[15] C.M. Davies, D.W. Dean, M. Yatomi, K.M. Nikbin, The influence of test duration and geometry on the creep crack initiation and growth behavior of 316H steel, material Science and engineering A, 510-511 (2009), pp. 202-206.
[16] H.F. Chen, Z. Z. Cen, B. Y. Yu, S. G. Zhan, A numerical method for reference stress in the evaluation of structure integrity, International Journal of Pressure Vessel and Piping, 71 81997), 47-53.
[17] F. Mueller, A. Scholz, C. Berger, Comparison of different approaches for estimation of creep crack initiation, Engineering Failure analysis 14 (2007) 1574-1585
[18] C.M. Davies, F. Mueller, K.M. Nikbin, N.P. O’Dowd, G.A.Webster, Journal of ASTM, International 3 (2) (2006), doi:10.1520/JAI13223.
[19] FITNET Fitness For Service (FFS) Procedure, vol II, ANNEX A, M Kocak, S. Webster, J.J. Janosch, R.A. Ainsworth, R. Koers, Editors, Revision MK8, 2008
[20] W. Sun, T.H. Hyde, A.A. Becker, J.A. Williams, Steady-state creep reference rupture stresses for internally pressurized pipes for use un life prediction, International Journal of pressure Vessel and Piping, 79 (2002) 135-143.
[21] British Energy Generation Ltd. “R6: Assessment of the Integrity of Structures Containing Defects”. British Energy Generation Ltd 1996. UK, Report R6, version 1.4, Appendix M7-6, pp: M7-3-5.
[22] British Energy Generation Ltd. R6: Assessment of the Integrity of Structures Containing Defects. British Energy Generation Ltd 2001. UK, Report R6, revision 4, Appendix IV.1.12.4, pp: IV.1.35.
[23] Fitness-For-Service, API579-1/ASME FFS-1, The American Society of Mechanical Engineers, June 5, 2007.
[24] Prager, M., “Development of the MPC Project Omega Method for Life Assessment in the Creep Range,” PVP-Vol. 288, ASME, 1994, pp. 401-421.